Available online at www.sciencedirect.com
ScienceDirect
Journal of Chromatography B, 852 (2007) 268–277
JOURNAL OF CHROMATOGRAPHY B
www.elsevier.com/locate/chromb

Shotgun analysis of phospholipids from mouse liver and brain by nanoflow liquid chromatography/tandem mass spectrometry

Dae Young Bang, Eun jeong Ahn, Myeong Hee Moon *

Department of Chemistry, Yonsei University, Seoul 120-749, South Korea

Received 10 November 2006; accepted 17 January 2007
Available online 1 February 2007

Abstract

It was demonstrated that a shotgun approach can be utilized for the characterization of phospholipids (PLs) extracted from mouse liver and brain by using nanoflow reversed phase liquid chromatography/electrospray ionization tandem mass spectrometry (LC–ESI-MS–MS). In this study, a dual scan method was introduced for the high throughput analysis of complex PL mixtures. Two consecutive LC–ESI-MS–MS runs were made in positive ion mode (for phosphatidylcholines (PCs) and phosphatidylethanolamines (PEs)) first followed by analysis in negative ion mode (for phosphatidylserine (PSs) and phosphatidylinositol (PIs)) using the same binary gradient elution with and without adding formic acid, respectively. The separation of the PLs was carried out using a home made pull tip capillary column (C18) with an end frit. The MS analysis of the eluted PL molecules was performed with a precursor scan followed by a data dependent MS–MS scan. The developed dual scan method was tested with the extracts of PCs and PIs mixtures from soybean, PEs from *Escherichia coli*, and PSs from bovine brain. It was further applied for the characterization of intact PL samples that were extracted from both mouse liver and mouse brain in the laboratory, and resulted in the identification of 90 and 80 PL species, respectively.

Keywords: Lipidomics; Phospholipids; Nanoflow liquid chromatography–tandem mass spectrometry; LC–MS–MS; Electrospray ionization; Mouse liver; Mouse brain

1. Introduction

Phospholipids (PLs) are present in all living organisms as building blocks of cellular membranes. The analysis of phospholipids has emerged as an active area of research in cellular biochemistry since compositional and structural determinations of the molecular lipid species play an important role in cellular metabolism, signal transduction, and membrane trafficking [1–3]. Due to advancements in mass spectrometry (MS), particularly with the introduction of the electrospray ionization (ESI) method, the analysis of phospholipids is now facilitated with an accurate and rapid determination of lipid structures aided by collision induced dissociation (CID) using tandem mass spectrometry [2,4–6]. Moreover, ESI-MS provides an improved sensitivity, low spectral background signals, and good compatibility with liquid chromatography (LC) [4,7]. The use of high performance liquid chromatography (HPLC) coupled with ESI-MS can increase the power of the characterization of PLs over gas chromatography since the combined LC–ESI-MS method can handle intact PLs without the need of derivatization [3,8–11].

While the separation and characterization of PLs have been investigated using LC–ESI-MS, it is not straightforward due to the limited capability of HPLC columns for the separation of different PL molecules since PLs are so diverse in their structures having different polar head groups, chain lengths and various degrees of unsaturation in the acyl chains. The separation of PLs on a normal phase LC (NPLC) column is mainly achieved based on the differences in the polar head groups of the PLs [12–15], whereas separation on a reversed phase LC (RPLC) column relies on the differences of chain length and the degree of unsaturation of the acyl chain [9,16]. Due to these limitations, single dimensional HPLC–ESI-MS alone has not provided a comprehensive analysis of complicated PL mixtures from biological organisms. Recently, an off-line two-dimensional HPLC method was reported to fractionate PLs

* Corresponding author. Tel.: +82 2 2123 5634; fax: +82 2 364 7050.
E-mail address: mhmoon@yonsei.ac.kr (M.H. Moon).

1570-0232/$ – see front matter © 2007 Elsevier B.V. All rights reserved.
doi:10.1016/j.jchromb.2007.01.028

by NPLC in the first dimension and the collected fractions were analyzed by RPLC–ESI-MS–MS using a C30 column [3]. The study demonstrated the identification of 110 PLs from rat liver.

In this study, a simple dual scan method was introduced for the selective identification of PL species using a shotgun RPLC–ESI-MS–MS method alone. In our earlier work [17], we have demonstrated the use of nanoflow LC–ESI-MS–MS in positive ion mode for the identification of intact PCs only from soybean, bovine brain and liver and the current study is expanded to characterize four PL species with a single capillary column. The developed method was based on two consecutive separations of the PLs by RPLC but the ESI-MS–MS was carried out in the positive ion mode for the first RPLC run followed by a data dependent MS-MS analysis, and then reanalyzed in the negative ion mode for the second run. With this method, phosphatidylcholine (PC) and phosphatidylethanolamine (PE) were predominantly detected in the positive ion mode, and phosphatidylserine (PS) and phosphatidylinositol (PI) were exclusively detected in the negative ion mode. The dual scan method in this study was evaluated with the PC and PI extracts from soybean, PEs from *Escherichia coli*, and PSs from bovine brain, and then was applied for the shotgun identification of intact PL mixtures from mouse liver and brain extracted in our laboratory.

2. Materials and methods

2.1. Materials

2.1.1. Standards and reagents

All standard phospholipids were purchased from Sigma–Aldrich (St. Louis, MO, USA): 18:0/18:1 PC, 16:0/16:0 PE, 16:0/18:2 PI, 16:0/16:0 PS, PC extracts (PCs) from soybean, PEs from *E. coli*, PSs from bovine brain, and PIs from soybean. The composition of PL species for these extracts were not known. For the RPLC column, capillary tubing (75 μm i.d., 360 μm o.d.) from Polymicro Technology LLC (Phoenix, AZ, USA) was used for packing the reversed phase resin (Magic C18, 5 μm–100 Å) obtained from Michrom BioResources Inc. (Auburn, CA, USA). All solvents (water, CH_3CN, CH_3OH, $CHCl_3$, and isopropanol) used were HPLC grade.

2.1.2. Lipid extraction

PLs were extracted from mouse liver and brain by the method of Bligh and Dyer [18]. For extraction, 0.4 g of mouse liver and 0.3 g of mouse brain were homogenized individually and each sample was vortexed under 0.75 mL of 1:2 (v/v) $CHCl_3$:CH_3OH. After vortexing, 0.25 mL of $CHCl_3$ was added and the solution was vortexed again. After adding 0.25 mL of distilled water and vortexing, the solution mixture was centrifuged at 13000 rpm for 5 min at room temperature. After a phase separation occurred, the bottom phase was recovered and dried. The final extract was re-dissolved in CH_3OH/CH_3CN (9:1) in preparation for HPLC separation.

2.2. Nanoflow LC–ESI-MS–MS

2.2.1. HPLC

The RPLC capillary column used in this study was packed in-house using a method that was explained in earlier reports [19,20]. One end of a silica capillary tube (150 mm × 75 μm i.d., 360 μm o.d.) was pulled by flame into a needle tip with an inner diameter of approximately 10 μm prior to packing. The tip was filled with a sol–gel frit of 1-mm length, as described previously [20]. The pulled-tip column with the end frit was packed with a methanol slurry of 5 μm 100 Å Magic C18 at a constant pressure (1000 psi) of He. The installation of end frit at the tip was to get a reproducible packing of capillary columns rather than a direct packing by forming a self assembled frit with packing materials. RPLC separation was carried out with a binary gradient elution using a model 1100 capillary pump system from Agilent Technologies (Palo Alto, CA, USA) which was equipped with an autosampler. The system configuration is illustrated in Fig. 1. During sample injection, the on–off valve connected to the PEEK microcross in Fig. 1 was closed so that the injection of the lipid sample (mostly with a 1-μL volume of sample solution) was made to the pulled tip column directly at 1 μL/min for 5 min. In order to fasten the sample loading, silica capillary tubing with a 50 μm i.d. was used to connect the binary pump to the microcross. After sample injection, a binary gradient elution began with the following mobile phase compositions: 50/50 CH_3CN/H_2O for solution A and 90/10 isopropanol/CH_3CN for B. For the positive ion mode of ESI-MS–MS, 0.1% formic acid was added to both mobile phase solutions, but for the negative

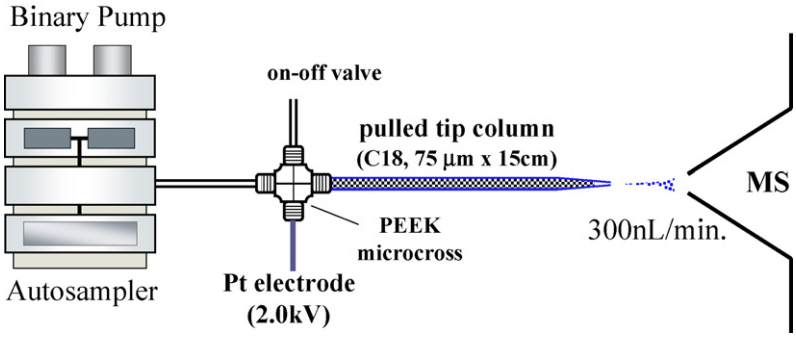

Fig. 1. Schematics of nanoflow LC–ESI-MS–MS with a pulled tip capillary column with the micro-tee connection for the application of voltage for electrospray ionization.

ion mode, formic acid was not added. The gradient elution conditions were varied based on the degree of complexity in the PL samples. Detailed gradient run conditions will be explained later in the results section. For gradient elution, a flow rate of 300 nL/min was maintained at the end of the column throughout all runs as the feed flow rate to the MS. However, from the binary pump to the PEEK microcross it was delivered at a relatively high speed (7 μL/min. of a total flow rate) and then the flow was divided into two directions at the microcross, with one part directed to an open vent valve and the other towards the analytical column. The flow rate was adjusted (300 nL/min) at the column outlet by controlling the length of vent tubing (25-μm i.d. capillary tubing). The flow splitting method was used mainly for minimizing delays of the gradient change by increasing the speed of flow delivery up to the microcross.

2.2.2. *Electrospray ionization tandem mass spectrometry*

An LCQ Deca ion trap mass spectrometer from Thermo Finnigan (San Jose, CA, USA) was utilized. Electrospray ionization was carried out at a potential of 2.0 kV applied via Pt wire and at a capillary temperature of 240 °C. The method of connecting Pt wire to the microcross along with a capillary column was explained in detail elsewhere [17,20]. While detecting PCs and PEs from PL mixtures, the positive ion mode of ESI was used. The negative ion mode was used to detect PSs and PIs. The acquisition of each mass spectrum was made with one precursor scan from 600 to 1000 amu with a mass tolerance of 1 U that was followed by a data-dependent MS–MS scan (45% normalized collision energy) using collision induced dissociation (CID) from 200 to 1000 amu. The acquired MS–MS spectra were analyzed manually using the *m/z* value determined from the precursor ion of the MS scan and their characteristic fragment ions from the CID spectrum.

3. Results and discussion

3.1. *Evaluation of the dual scan method for nanoflow LC–ESI-MS–MS for PL standards*

The dual scan method (scanning in positive and negative ion modes) has been tested with a mixture of four different standard phospholipids (18:1/18:1-PE, 18:0/18:1-PC, 16:0/18:2-PI and 16:0/16:0-PS) by nanoflow LC–ESI-MS–MS. Fig. 2 shows the base peak chromatograms (BPCs) of the PL standard mixtures (1.0 ng for each standard) obtained with nanoflow LC followed by a precursor scan and then a data dependent MS–MS scan via ion trap MS. The binary gradient elution began at 70% B and ramped to 80% B over 5 min and was then maintained at this level. The first RPLC run (Fig. 2a) was carried out in the positive ion mode of the ESI and the same gradient RPLC run was repeated but analyzed in negative ion mode (Fig. 2b). While PC and PE were successfully detected in positive ion mode as shown in Fig. 2a, PI and PS were detected ~30 times (shown at an enlarged scale around 10 min.) less than PC and PE in a direct comparison of peak intensities. When the mobile phases were slightly acidic (0.1% formic acid added), it was expected that neutral lipids, such as PC and PE would be preferably protonated, but negatively charged lipids, such as PI and PS would hardly appear to be charged into positive ions. However, when the negative ion mode was employed for the second RPLC–ESI-MS run, this phenomenon was reversed, as shown in Fig. 2b. It was noted that PC and PE were undetected in negative ion mode (the amounts injected for both runs were the same) while PI and PS were predominantly detected. When the peak intensity of PI in the negative ion mode was directly compared from that obtained in the positive ion mode, it showed approximately 150 times high intensity in the negative ion mode. Based on the limit of detection (LOD) for the current nanoflow LC–MS setup, which was found to be 2.4 ng/mL for 14:0/14:0-PC in a previous study [17], the injection amounts of PL standards used to generate data in Fig. 2 were set to be high enough for detection. It was thought that PC and PE were not properly ionized in negative ion mode under the neutral mobile phase solutions used, and thus were undetectable.

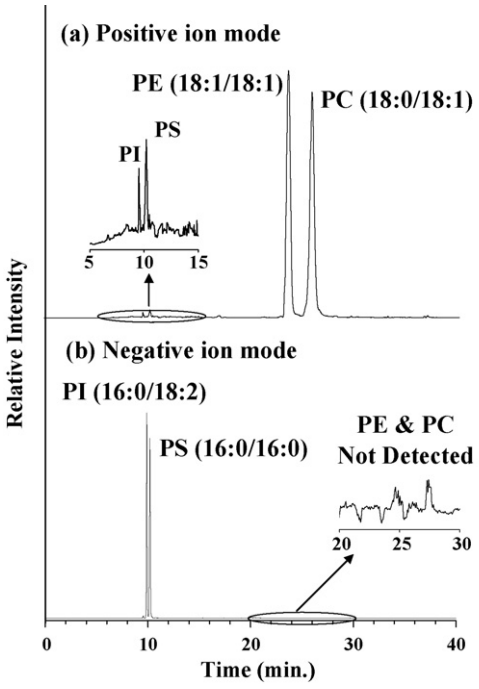

Fig. 2. Base peak chromatograms of standard phospholipids mixtures with nanoflow LC followed by precursor scans at (a) positive and at (b) negative ionization mode. Both scans were obtained at the same binary gradient RPLC run: binary gradient began at 70% of mobile phase B and ramped to 80% for 5 min and then maintained (mobile phase A: 50/50 CH_3CN/water, B: 90/10 isopropanol/CH_3CN). Formic acid (0.1%, v/v) is added to both mobile phases for positive ion mode runs only.

Each standard phsospholipid molecule that eluted from the LC run was detected first by a precursor scan and was then followed by data-dependent MS–MS fragmentation. The CID spectra of the PE and PC standards obtained in the positive ion mode in Fig. 3a and b show the fragment ions, *m/z* 603.9 of $[M+H-141]^+$ for 18:1/18:1-PE and *m/z* 605.9 of $[M+H-183]^+$ for 18:0/18:1-PC, representing the loss of polar head groups, $HPO_4(CH_2)_2NH_3$ (141 amu) and $HPO_4(CH_2)_2N(CH_3)_3$ (183 amu), respectively[5,21]. Molecular ion peak ($[M+H]^+$) of PE in the positive ion mode was not observed in our CID experiment (the *m/z* of the molec-

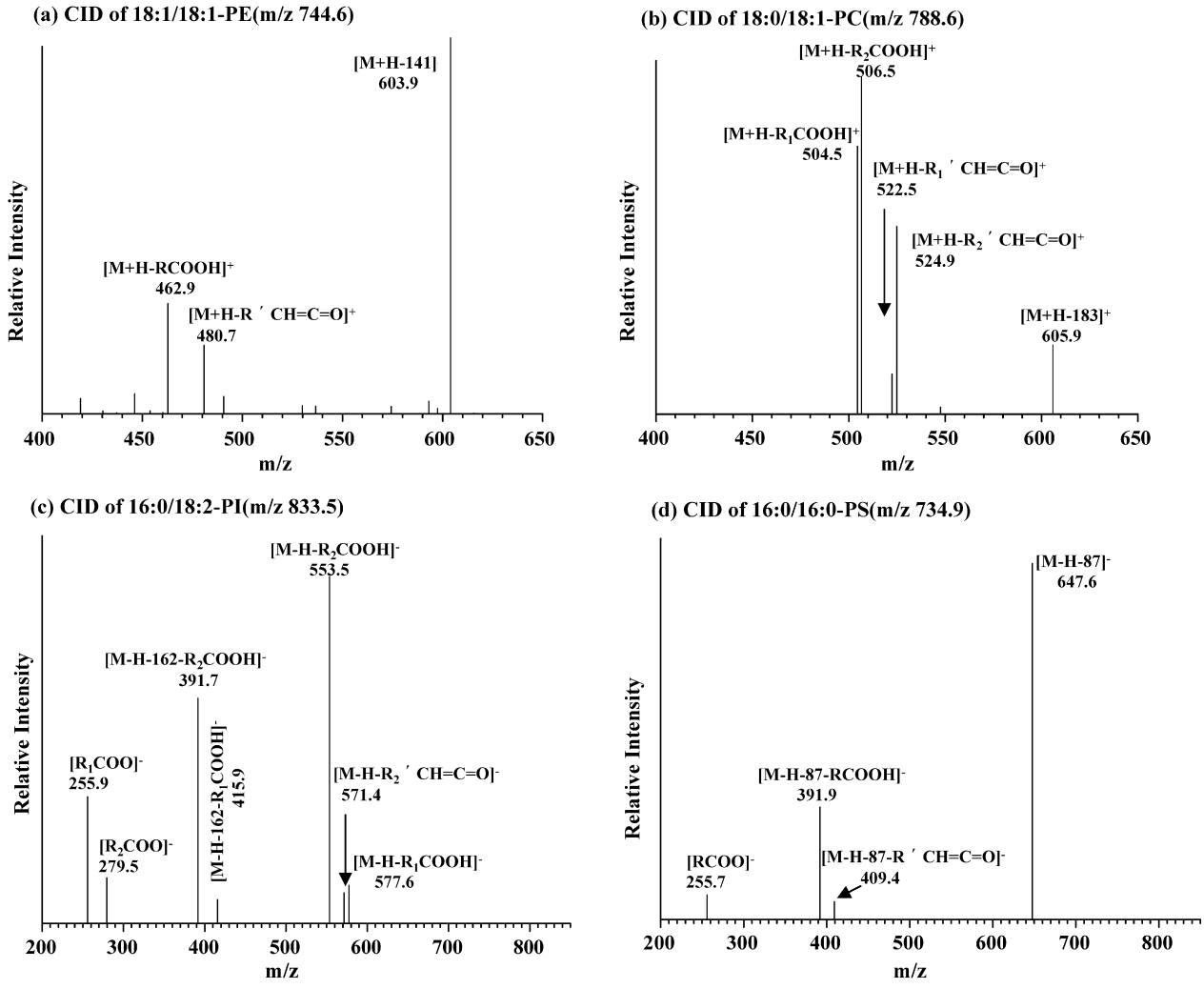

Fig. 3. CID spectra of standard PL species during nanoflow LC–ESI-MS–MS runs in Fig. 2 obtained at positive ion mode (a) 18:1/18:1-PE and (b) 18:0/18:1-PC and at negative ion mode (c) 16:0/18:2-PI and (d) 16:0/16:0-PS.

ular ion was confirmed in a precursor scan just prior to the data dependent CID) due to a proper adjustment of collision energy to enhance fragmentation. The CID spectrum of 18:1/18:1-PE in Fig. 3a clearly shows fragment ions at *m/z* 480.7 and *m/z* 462.9, corresponding to the loss of a fatty acid in the form of a ketene ($[M+H-R'CH{=}C{=}O]^+$) and a carboxylic acid ($[M+H-RCOOH]^+$), respectively. In the case of 18:0/18:1-PC in Fig. 3b, the characteristic fragment ions corresponding to the loss of a fatty-acid in the form of ketene appear at *m/z* 522.5 $[M+H-R'_1CH{=}C{=}O]^+$ and *m/z* 524.9 $[M+H-R'_2CH{=}C{=}O]^+$ with the latter ion occurring in greater abundance, which helps identifying the location of double bond at *sn*-2 position.

The CID spectra of 16:0/18:2-PI and 16:0/16:0-PS display the typical characteristic fragment ions that can be obtained in negative ion mode as well as similar fragmentation patterns to those observed in PE and PC. PI produces typical fragment ions that reflected the loss of a fatty acyl moiety as *m/z* 577.6 for $[M-H-R_1COOH]^-$, *m/z* 553.5 for $[M-H-R_2COOH]^-$ with the latter fragment ion more abundant. While Fig. 3c showed the fragment ion peak of the neutral loss of acyl chain in the form of ketene $[M-H-R'_2CH{=}C{=}O]^-$ at *m/z* 571.4, a similar fragment ion peak representing the loss of ketene from *sn*-1 acyl chain was not observed due to the relatively low intensity. Collision energy for CID experiment in the negative mode was not set to observe molecular ion peak ($[M-H]^-$) of PI, either. The characteristic features used to identify PI from Fig. 3c were the appearance of ions at *m/z* 415.9 ($[M-H]^- - 162 - R_1COOH$) and *m/z* 391.7 ($[M-H]^- - 162 - R_2COOH$) which arose from the respective loss of the fatty acid at *sn*-1 and at *sn*-2 from ions of $[M-H-162]^-$ that resulted from the loss of the inositol head group (162 Da). In addition, the $R_1CO_2^-$ ion located at *m/z* 255.9 and the $R_2CO_2^-$ ion located at *m/z* 279.5 are also characteristic ions used to identify the fatty-acyl chains. It was also noted that the $R_1CO_2^-$ anion was more abundant than the $R_2CO_2^-$ anion in our experiment. A much simpler CID fragmentation spectrum was obtained with 16:0/16:0-PS in Fig. 3d due to the identical fatty acyl chains. However, PS produced a prominent and characteristic $[M-H-87]^-$ ion at *m/z* 647.6, which supported the conclusion that the serine head group (loss of $C_3H_5NO_2$, 87 Da) is labile [22]. This was also supported by

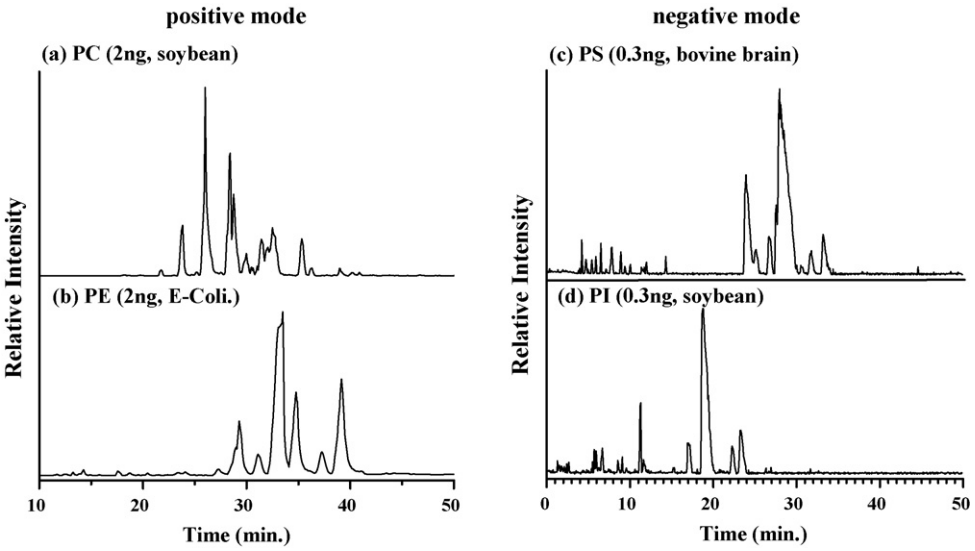

Fig. 4. Base peak chromatograms of (a) soybean PC extracts and (b) *E. coli*. PE extracts which were obtained at positive ion mode, and BPCs of (c) bovine brain PC extracts and (d) soybean PI extracts at negative ion mode. Binary gradient elution conditions for positive ion mode begins at 50% of mobile phase B and ramps to 70% of B for 40 min and then maintains at 70%. For negative mode, binary condition begins at 60% B, ramps to 80% for 40 min and then fixed. Mobile phase compositions are the same as used in Fig. 2.

ions at *m/z* 391.9 ($[M-H-87-RCOOH]^-$) and *m/z* 409.4 ($[M-H-87-R'CH{=}C{=}O]^-$), which show each fragment ion corresponding to the neutral loss of fatty-acyl chain in the form of an acid and a ketene, respectively, from the $[M-H-87]^-$ ion rather than directly from original molecular ion ($[M-H]^-$).

3.2. Characterization of PC, PE, PS, and PI extracts

The current nanoflow LC–ESI-MS–MS method has been tested with four different phospholipid samples: PCs from soybean, PEs from *E. coli*, PSs from bovine brain, and PIs from soybean. Fig. 4 represents the four base peak chromatograms of (a) PCs and (b) PEs obtained in the positive ion mode and of (c) PSs and (d) PIs in the negative ion mode. The mobile phase compositions utilized for the RPLC separation in Fig. 4 were the same as used for Fig. 2. However, the binary gradient elution conditions for positive ion mode began at 50% B and ramped to 70% B over 40 min, at which level it was then maintained. The binary gradient elution conditions for negative ion mode (Fig. 4c and d) began at 60% B, ramped to 80% over 40 min and then were maintained at 80% B until the end of the run. The data dependent CID analysis yielded the identification of 23 PC molecules from Run a, 9 PE species from Run b, 19 PS species from Run c, and 19 PI species from Run d. All identified PL molecules are listed in Table 1 along with the relative peak area calculated from the area of each extracted chromatogram. Though the values of the relative peak area do not represent accurate information of the concentration differences, they can provide an overview of the relative differences in the peak area among the species. A correction for the difference of ionization efficiencies among each PL series depending on the carbon chain number was not included in this study and will be integrated in the near future. It was noted that 2 ng each of PC and PE samples was injected for separation; however, only 0.3 ng each of the PS and PI samples were utilized in negative ion mode. This revealed that ionization in negative ion mode was more sensitive than that for positive ion mode.

3.3. Shotgun analysis of intact PLs from mouse liver and brain

The dual scan nanoflow LC–ESI-MS–MS method was applied for the shotgun characterization of phospholipid mixtures extracted from mouse liver and brain. The two base peak chromatograms shown in Fig. 5a and b were obtained from two consecutive LC runs for the mouse liver extracts carried out in positive and negative ion modes. A binary gradient condition extended more than that of Fig. 4 in order to handle complicated PL mixtures was applied as follows: it began at 30% B, ramped to 55% B over 20 min, increased to 65% B over 40 min, increased to 90% B over 10 min, and was finally maintained at 90% B until the end of the run. The amounts injected for the PL mixtures were approximately 90 and 9 ng for Runs a and b, respectively. The reduction of injection amount for negative ion mode was based on the results from the experiments with standard PL extracts shown in Fig. 4. When the MS spectrum of a precursor scan was extracted from a retention time of 48.53 min (marked as * in Fig. 5a), it was found to exhibit five distinctive ion peaks of *m/z* 716.9, *m/z* 740.5, *m/z* 767.1, *m/z* 784.8 and *m/z* 809.0 as seen in Fig. 6a. The data dependent CID spectra of *m/z* 784.8 and 740.5 were shown in Fig. 6b and c, respectively. Fig. 6b was identified as 16:0/20:3-PC from the characteristic $[M+H-183]^+$ ion at *m/z* 601.6 along with the ions of *m/z* 528.7 and *m/z* 478.5 reflecting the loss of carboxylic acids at *sn*-1 and *sn*-2, respectively, and the ions of *m/z* 546.8 and *m/z* 496.4 representing the loss of a ketene from both acyl chains. The CID spectrum of the molecular ion having *m/z* 740.5 was identified as 16:0/20:4-PE from the assigned fragment ions shown in Fig. 6c. The other

Table 1
Identified phospholipids (PCs from soybean, PEs from E.Coli, PSs from bovine brain, and PIs from soybean) by nanoflow LC–ESI-MS–MS shown in Fig. 4

Molecular species	*m/z*	t_r (min)	Relative area (%)
PCs from soybean			
18:3/18:3	778.6	21.75	0.70
14:0/18:3	728.5	22.65	0.04
16:1/18:3	754.6	22.98	0.07
18:2/18:3	780.8	23.83	7.61
14:0/18:2	730.7	24.66	0.16
16:1/18:2	756.6	26.02	0.51
18:2/18:2	782.8	26.02	21.08
18:1/18:3	782.8	26.37	4.22
16:0/18:2	758.8	28.41	16.79
18:1/18:2	784.9	28.74	13.00
18:0/18:3	784.9	29.97	3.87
16:0/16:0	734.9	30.88	0.73
16:0/18:1	762.5	31.43	6.56
18:1/18:1	786.9	32.05	9.06
18:0/18:2	786.9	32.5	7.26
18:0/18:1	788.7	35.31	6.13
20:0/18:2	814.7	36.23	1.12
22:0/18:3	840.7	37.39	0.05
18:0/18:0	790.7	38.01	0.08
20:0/18:1	816.8	38.33	0.12
22:0/18:2	842.6	39.09	0.58
23:0/18:2	856.6	40.07	0.12
24:0/18:2	870.6	41.38	0.11
PSs from bovine brain			
18:0/21:6	820.6	20.87	1.71
22:4/22:6	882.6	21.74	0.56
18:0/20:6	806.8	21.94	0.39
18:1/22:6	832.7	22.07	1.05
16:0/24:6	834.8	22.34	3.06
18:0/22:6	834.8	23.92	9.86
16:0/18:1	760.6	24.53	0.10
18:1/18:1	786.6	25.13	3.97
18:0/20:4	810.7	25.6	0.22
18:0/22:5	836.8	26.62	4.45
18:0/22:4	838.7	27.56	5.92
18:0/18:1	788.9	27.96	57.79
18:1/20:1	814.6	29.03	0.46
18:0/20:2	814.6	30.51	0.84
18:0/22:3	840.6	31.77	2.80
18:0/24:4	866.7	31.97	0.19
18:0/20:1	816.5	33.19	5.52
18:0/22:2	842.7	33.59	1.05
18:0/22:1	844.6	38.47	0.05
PEs from *E.coli*			
14:0/16:1	662.8	24.08	1.22
16:1/16:1	688.8	24.08	0.46
16:0/14:0	664.7	28.06	13.91
16:0/16:1	690.5	28.99	16.76
16:1/18:1	716.8	31.06	3.81
16:0/18:1	718.9	34.77	45.45
16:0/16:0	692.8	34.91	11.69
20:0/16:1	746.6	41.02	4.04
16:0/18:0	720.5	41.24	2.66
PIs from soybean			
18:3/18:3	853.4	14.32	1.18
16:1/18:3	829.4	15.12	0.11
18:2/18:3	855.5	15.32	0.56
14:0/18:2	805.1	16.81	0.04
16:0/18:3	831.1	16.98	5.02
18:2/18:2	857.1	17.12	0.48
16:0/16:1	807.1	17.68	0.20
16:0/18:2	833.4	18.66	58.46
18:1/18:2	859.4	20.11	0.46
18:0/18:3	859.4	20.68	1.02
16:0/18:1	835.4	22.21	4.87
18:0/20:4	885.2	22.64	0.15
18:0/18:2	861.4	23.28	9.95
16:0/18:0	837.2	23.72	0.48
18:0/18:1	863.2	24.97	15.10
20:0/18:2	889.2	26.12	0.65
22:0/18:2	917.1	27.12	0.73
23:0/18:2	931.2	28.65	0.26
24:0/18:2	945.4	29.27	0.26

Each species are listed with its retention time (t_r) and relative peak area observed from each extracted chromatogram.

three ions (*m/z* 716.9, 767.1 and 809.0) in Fig. 6a were identified as 16:0/18:2-PE, 18:1/20:4-PE, and 18:0/20:5-PC, respectively, from their CID spectra (data not shown). Since the precursor ion detection and subsequent CID experiment shown at Fig. 6 were carried out when BPC chromatogram of Fig. 5a approached to nearly the baseline level, it demonstrated the efficiency of the current nanoflow LC–ESI-MS–MS experiment for separation and simultaneous characterization of a small amount of PL mixtures.

During the second LC run in negative ion mode, PS and PI molecules were identified as detailed above. The precursor scan at 45.78 min (marked as **) of Fig. 5b shows three distinctive ions in the *m/z* range of 700–950 as shown in Fig. 7a. From each individual CID spectrum obtained by the data dependent MS-MS experiments, two PIs and one PS were identified at the given time frame (45.78 min). For the case of the ion *m/z* 885.2

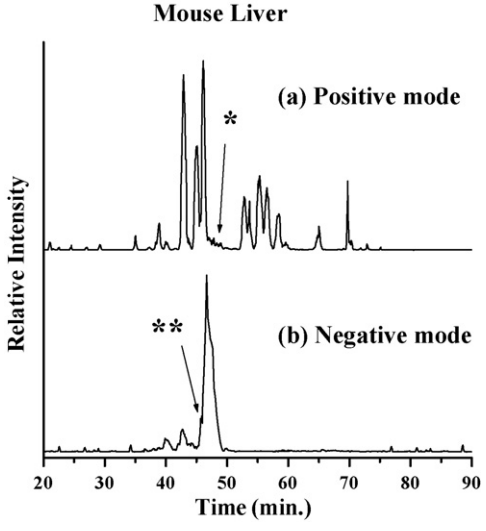

Fig. 5. Base peak chromatograms of intact phospholipids extracted from mouse liver at (a) positive and (b) negative ion mode by nanoflow LC–ESI-MS–MS. A same binary gradient elution condition for both positive and negative ion mode begins at 30% of mobile phase B and ramps to 55% of B for 20 min, to 65% for 40 min, to 90% for 10 min and the fixed. Mobile phase compositions are the same as used in Fig. 4. CID experiments at the time frames marked with asterisks shown on both BPCs are explained at the following figures.

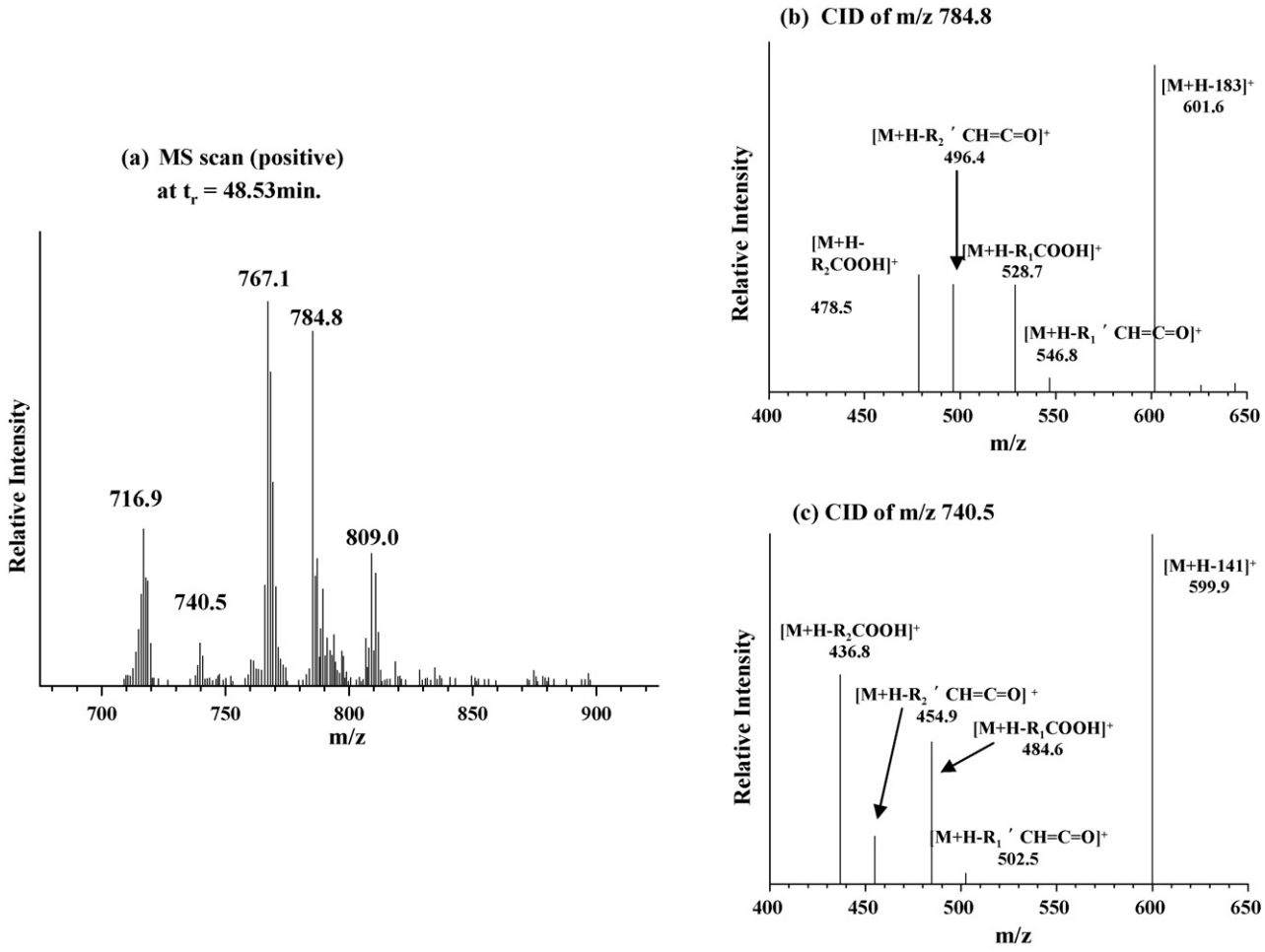

Fig. 6. (a) A precursor MS scan at positive ion mode at t_r = 48.53 min (marked as * in Fig. 5a), (b) CID spectrum of *m/z* 784.8 (identified as 16:0/20:3-PC), and (c) CID spectrum of *m/z* 740.5 (identified as 16:0/20:4-PE obtained by nanoflow LC–ESI-MS–MS.

in Fig. 7a, it was identified as 18:0/20:4-PI from the fragmentation pattern shown in Fig. 7b. The CID spectrum contains the characteristic ions of $[M - H - 162 - RCOOH]^-$ (*m/z* 439.8 for R_1 and *m/z* 419.4 for R_2) and the two carboxylate anions at *m/z* 283.2 and *m/z* 303.6. The fragmentation of *m/z* 834.5 leads to an identification of 18:0/22:6-PS along with the fragment ions assigned in Fig. 7c. In the dual scan experiment, a total of 90 PL species (42 PCs, 18 PEs, 16 PSs, and 14 PIs) were identified from the mouse liver. This number was somewhat less than the results (110 PLs from rat liver) obtained by an off-line 2D-LC–ESI-MS–MS method [3]. The current method offers an advantage of analyzing small amount of PL mixtures without an off-line collection of LC fractions for a secondary LC run, however it requires two repeated LC runs.

The same experimental scheme was applied to another PL mixture sample extracted from mouse brain, and their BPCs are shown in Fig. 8. Experiments were carried out using the same gradient run conditions as described for Fig. 5, but the injection amounts (for LC runs) were approximately 80 and 8 ng for the positive and negative ion modes, respectively. The mouse brain sample analysis resulted in the identification of a total of 80 phospholipids: 32 PCs, 16 PEs, 23 PSs, and 9 PIs. These are listed in Table 2 together with data from liver. The injection amount, 8 ng for the negative ion mode, was optimized to achieve maximum identification of PIs and PSs due to ion suppression effects by the very abundant species (18:0/22:6-PS and 16:0/18:1-PI) which eluted together at 43–45 min. The relative peak area of 18:0/22:6-PS occupied approximately 81% based on the calculation of each peak area without considering the dependency of peak intensity on the carbon numbers of lipid molecules. This observation is similar to the results of brain lipid standard extracts examined in Table 1. For the case of PSs listed in Table 1, very few number of PS molecules occupy the majority of entire PS species: 18:0/18:1 and 18:0/22:6.

In Table 2, relative peak area values of identified PL species are not included since comparison of peak area among different head group species is more complicated. Instead, the PL species are compared from the different organs and they are listed in an increasing order of retention time. By directly comparing the compositional distribution, there is a clear difference in the molecular compositions between liver and brain. Since the LC–ESI-MS–MS runs for both samples were obtained with the use of two different batch of home made capillary LC columns, the retention time of each molecular species from liver and brain samples can be different slightly. However, the difference in retention time is less than 2% in maximum.

Table 2
Identified phospholipids from mouse liver and brain by nanoflow LC–ESI-MS–MS shown in Figs. 5 and 8, respectively

Class	Molecular species	*m/z*	t_r (min)	
			Liver	Brain
Positive mode				
PC	14:0/16:0	706.6		32.63
	16:1/20:5	778.5	33.51	
	14:0/20:4	754.6	34.26	
	16:1/22:6	804.7	35.13	
	18:3/18:2	780.5	36.33	
	18:1/18:4	780.5	36.86	
	18:2/22:6	830.6	37.15	
	14:0/18:2	730.5	37.15	
	16:1/20:4	780.7	37.23	
	16:0/20:5	780.8	38.08	
	16:2/18:1	756.6	38.24	
	16:1/18:2	756.6	38.55	
	16:0/18:3	756.6	38.76	
	18:2/20:4	806.6	38.9	38.77
	18:4/18:1	780.8		39.06
	18:2/18:2	782.6	39.32	
	16:1/20:3	782.6	40.22	
	22:6/16:0	806.7		41.99
	16:0/22:6	806.7	42.88	42.93
	18:1/22:6	832.5	43.53	43.28
	16:0/16:1	732.7	43.97	43.64
	16:0/20:4	782.7	45.11	44.87
	18:1/20:4	808.8	45.21	45.54
	16:1/18:1	758.8	45.62	
	16:0/22:5	808.8	45.66	45.54
	16:0/18:2	758.7	46.36	45.83
	18:1/22:5	834.5		46.32
	16:0/20:3	784.6	48.03	48.23
	18:1/18:2	784.6	48.53	48.73
	18:0/20:5	808.8	48.89	
	18:0/18:3	784.6	48.95	
	16:0/22:4	810.5		50.01
	18:1/20:3	810.5		51.05
	16:0/16:0	734.6	52.36	52.41
	18:1/16:0	760.8		52.66
	16:0/18:1	760.8		52.77
	18:0/22:6	834.6	52.78	52.77
	16:0/18:1	760.6	53.39	
	18:1/18:1	786.7	54.33	54.42
	18:0/20:4	810.5	55.33	55.34
	16:0/18:0	762.6	55.89	
	18:0/16:0	762.6	55.97	
	16:0/20:2	786.7	55.97	
	18:0/22:5	836.8		56.04
	18:0/18:2	786.7	57.01	
	18:0/22:5	836.6	57.73	
	18:0/20:3	812.7	59.73	59.21
	18:0/22:4	838.8	63.06	62.62
	18:0/16:0	762.6		62.68
	16:0/18:0	762.6		63.21
	20:1/16:0	788.6		63.71
	18:0/18:1	788.7	64.68	64.53
	18:0/20:2	814.9		65.86
	18:0/22:3	840.7		66.43
	18:0/18:0	790.5	67.73	67.45
	20:0/18:2	814.8	70.88	
PE	22:6/22:6	836.7		35.56
	18:0/18:6	736.6	36.98	
	18:2/22:6	788.9		37.71
	20:4/22:6	812.6		37.79
	16:1/22:6	762.5		38.33
	22:3/18:5	788.9		38.93
	18:3/20:4	762.7	41.46	
	18:1/18:5	736.5	41.73	
	18:1/20:5	764.7	45.5	
	16:0/22:6	764.7	45.71	45.4
	18:2/22:5	790.7		46.22
	16:0/20:4	740.5	47.48	47.32
	16:0/18:2	716.8	48.07	
	18:2/20:4	764.7	48.28	
	18:1/20:4	766.7	48.47	48.16
	18:1/16:0	718.8	49.69	
	16:0/18:1	718.8	49.79	
	18:0/22:5	794.7	51.28	
	18:0/22:6	792.6		56.04
	18:0/16:1	718.7		56.68
	18:0/18:2	744.8		57.77
	18:0/20:4	768.5	58.31	58.24
	18:1/18:1	744.5	59.67	
	16:0/20:1	746.8		59.83
	18:0/22:4	796.5		65.38
	20:3/18:0	770.6	62.01	
	18:0/20:3	770.6	62.66	
	20:0/20:5	794.7	62.85	
	18:0/18:1	746.7	67.27	66.85
Negative mode				
PS	22:6/22:6	878.8		35.09
	20:4/22:6	854.6	36.47	36.18
	22:5/22:6	880.5		36.87
	22:6/18:2	831.0	36.87	
	18:2/22:6	830.9		37.07
	20:4/20:4	831.0	37.51	
	20:4/18:2	806.8	38.09	
	22:4/22:6	882.6		39.55
	16:0/22:6	806.8	39.91	39.92
	18:1/22:6	832.7	39.98	40.32
	20:3/22:6	856.6		40.52
	18:1/20:4	808.7		41.60
	16:0/20:4	782.7	41.72	
	18:0/22:6	834.7	44.51	43.79
	18:0/20:5	808.8	44.97	
	16:0/18:1	760.7		43.79
	18:1/18:1	786.7		45.67
	16:0/18:0	762.7		45.91
	18:0/20:4	810.8	50.51	50.05
	18:0/20:3	812.8	52.95	53.62
	18:0/22:5	836.6	53.15	53.89
	18:0/22:4	838.9	53.38	54.02
	18:0/24:6	862.7	54.13	
	20:0/22:6	862.7	54.47	
	18:0/18:1	788.8	58.40	57.72
	18:0/20:2	814.9		58.08
	18:0/18:0	790.8		58.93
	18:0/22:3	840.5		63.96
	18:0/20:1	816.7		65.82
	22:0/18:1	844.8		74.72
PI	18:2/20:4	881.3		38.30
	16:0/22:6	881.4	40.19	39.78
	16:0/20:4	857.3	41.52	40.92
	16:1/18:1	833.2		40.92
	18:1/20:4	883.3	41.85	41.47
	18:0/20:5	883.3		42.74

Table 2 (*Continued*)

Class	Molecular species	*m/z*	t_r (min)	
			Liver	Brain
	16:0/18:1	835.1	43.92	43.05
	18:0/22:6	909.5		43.32
	16:0/18:2	833.3	44.49	
	18:1/18:2	859.5	44.97	
	18:0/20:5	883.4	45.08	
	18:0/22:6	909.4	45.93	
	18:0/20:4	885.4	46.65	45.74
	18:1/18:1	861.4	46.88	
	18:0/18:2	861.4	53.98	
	18:0/20:3	887.3	54.41	
	18:0/22:4	913.2	55.03	
	20:0/20:4	913.2	57.35	

PCs and PEs were identified at positive ion mode of data dependent CID from nanoflow LC–ESI-MS–MS, and PSs and PIs were at negative ion mode.

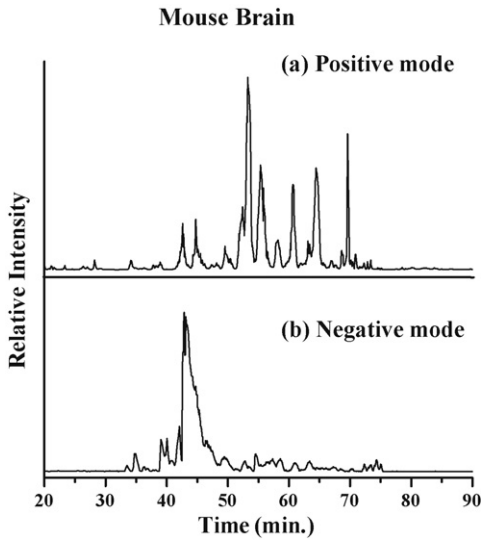

Fig. 8. Base peak chromatograms of intact phospholipids extracted from mouse brain at (a) positive and (b) negative ion mode by nanoflow LC–ESI-MS–MS. A binary gradient elution condition used for both positive and negative ion mode is the same as used in Fig. 5.

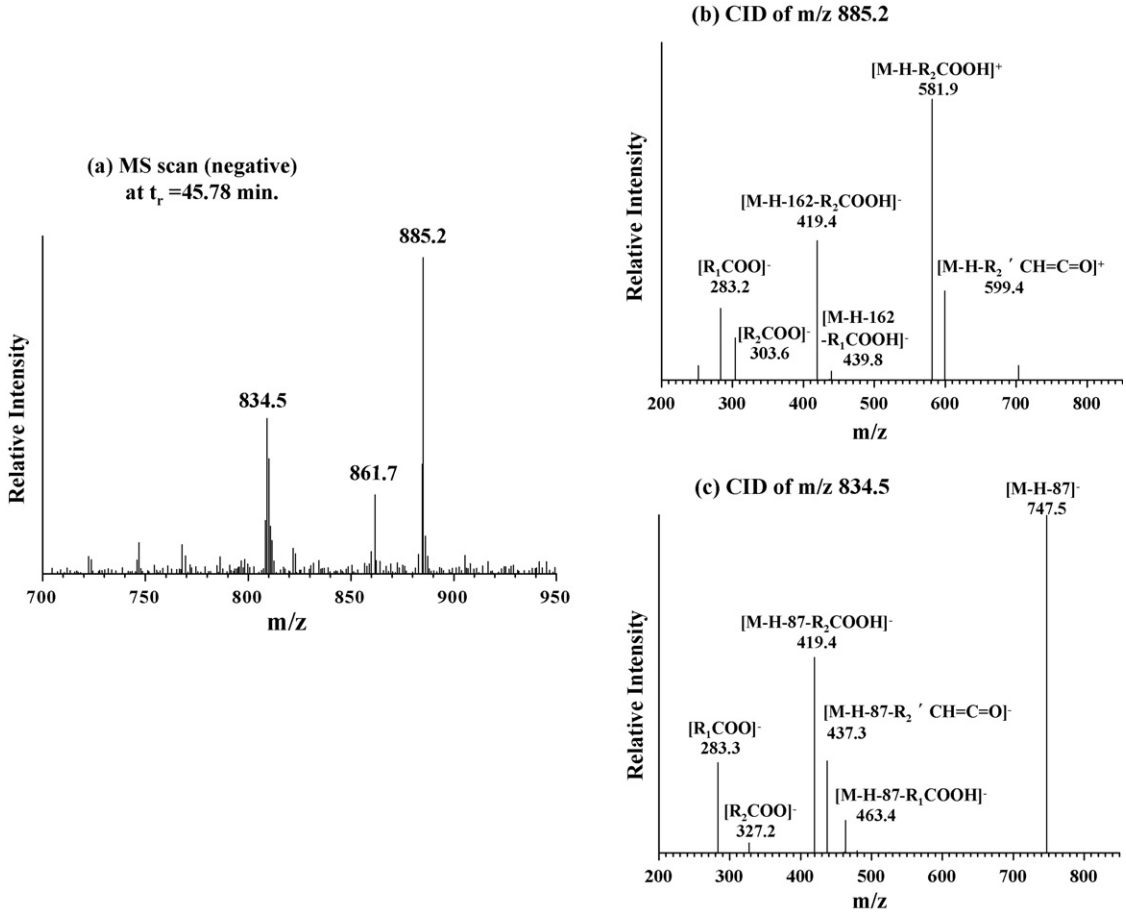

Fig. 7. (a) A precursor MS scan at negative ion mode at t_r = 45.78 min (marked as ** in Fig. 5b), (b) CID spectrum of *m/z* 885.5 (identified as 18:0/20:4-PI), and (c) CID spectrum of *m/z* 834.5 (identified as 18:0/22:6-PS) obtained by nanoflow LC–ESI-MS–MS.

4. Conclusions

In this study, we reported the potential applicability of a nanoflow LC–ESI-MS–MS method for the shotgun identification of phospholipids in mouse liver and brain tissues. This study described a simple but powerful new method for characterizing PLs by introducing a dual scan method in which RPLC separation is carried out repeatedly but at different ionization modes. The shotgun method employed here requires only a single dimensional RPLC column operated using the same gradient elution conditions for both LC runs. By employing the data dependent CID fragmentation experiments after each precursor scan of ESI-MS, the identification of chain length and structure of the PLs can be made without ambiguity. It was also noted that LC–ESI-MS–MS of the PLs in negative ion mode had an MS intensity that was about ten times higher than was observed in positive ion mode.

A limitation of the current work at this stage is the lack of an automated database search program to distinguish the different PL species from each CID spectra. The current study was conducted by searching each PL species by manually comparing the CID pattern obtained experimentally with the known characteristic fragment ions for each PL species. Further study is needed to quantitatively identify the relative abundance of the different PL species using an internal standard method which compensates for the differences in the ionization efficiency of the PLs according to their carbon numbers. With the employment of a quantitative identification method, this nanoflow LC–ESI-MS–MS could be used for the determination of the relative variation of PL species as dependent on the stages of disease or cell growth.

Acknowledgements

This study was supported by a grant (2006-04006) from the Korea Ministry of Science & Technology (MOST) and partly by a grant from the Korea Science and Engineering Foundation through the Center for Bioactive Molecular Hybrids (CBMH). The authors also thank to ProteomeTech Inc. for the access to the MS facility.

References

[1] J.F.H.M. Brouwers, E.A.A.M. Vernooji, A.G.M. Tielens, L.M.G. van Golde, J. Lipid Res. 40 (1999) 164.
[2] M. Pulfer, R.C. Murphy, Mass Spectrom. Rev. 22 (2003) 332.
[3] T. Houjou, K. Yamatani, M. Imagawa, T. Shimizu, R. Taguchi, Rapid Commun. Mass Spectrom. 19 (2005) 654.
[4] X. Han, R.W. Gross, J. Am. Soc. Mass Spectrom. 6 (1995) 1202.
[5] F.-F. Hsu, J. Turk, J. Am. Soc. Mass Spectrom. 14 (2003) 352.
[6] T. Houjou, K. Yamatani, H. Nakanishi, M. Imagawa, T. Shimizu, R. Taguchi, Rapid Commun. Mass Spectrom. 18 (2004) 3123.
[7] H.-Y. Kim, T.-C.L. Wang, Y.-C. Ma, Anal. Chem. 66 (1994) 3977.
[8] J. Fang, M.J. Barcelona, J. Microbiol. Methods 33 (1998) 23.
[9] C.A. Lytle, Y.D. Gan, D.C. White, J. Microbiol. Methods 41 (2000) 227.
[10] R. Taguchi, J. Hayakawa, Y. Takeuchi, M. Ishida, J. Mass Spectra 35 (2000) 953.
[11] G. Isaac, D. Bylund, J.-E. Mansson, K.E. Markides, J. Borgquist, J. Neurosci. Methods 128 (2003) 111.
[12] W.W. Christie, J. Lipid Res. 26 (1985) 507.
[13] J. Becart, C. Chevailer, J.P. Biesse, J. High Resolut. Chromatogr. 13 (1990) 126.
[14] C.J. DeLong, P.R.S. Baker, M. Samuel, Z. Cui, M.J. Thomas, J. Lipid Res. 42 (2001) 1959.
[15] J. Hayakawa, Y. Okabayashi, J. Pharm. Biomed. Anal. 35 (2004) 583.
[16] G.M. Patton, J.M. Fasulo, S.J. Robins, J. Lipid Res. 23 (1982) 190.
[17] D.Y. Bang, D. Kang, M.H. Moon, J. Chromatogr. A. 1089 (2005) 203.
[18] E.G. Bligh, W.J. Dyer, Can. J. Biochem. Physiol. 37 (1959) 811.
[19] M.H. Moon, S. Myung, M. Plasencia, A.E. Hilderbrand, D.E. Clemmer, J. Proteome Res. 2 (2003) 589.
[20] D. Kang, H. Nam, Y.-S. Kim, M.H. Moon, J. Chromatogr. A 1070 (2005) 193.
[21] J.L. Kerwinm, A.R. Tuininga, L.H. Ericsson, J. Lipid Res. 35 (1994) 1102.
[22] F.-F. Hsu, J. Turk, J. Am. Soc. Mass Spectrom. 15 (2005) 1510.